High Efficiency Silicon Module Degradation - From Atoms to Systems

Preprint

D.C. Jordan,[1] D.B. Sulas-Kern,[1] S. Johnston,[1]
H.R. Moutinho,[1] C. Xiao,[1] C.S. Jiang,[1] M. Young,[1]
A.G. Norman,[1] C. Deline,[1] I. Repins,[1] R. Bhoopathy,[2]
O. Kunz,[2] Z. Hameiri,[2] C. Sainsbury[3]

1 National Renewable Energy Laboratory
2 USNW Australia
3 Sinton Instruments

Presented at the 37th European Photovoltaic Solar Energy Conference and Exhibition (EU PVSEC 2020)
September 7-11, 2020

NREL is a national laboratory of the U.S. Department of Energy
Office of Energy Efficiency & Renewable Energy
Operated by the Alliance for Sustainable Energy, LLC

This report is available at no cost from the National Renewable Energy Laboratory (NREL) at www.nrel.gov/publications.

Contract No. DE-AC36-08GO28308

Conference Paper
NREL/CP-5K00-77483
September 2020

High Efficiency Silicon Module Degradation - From Atoms to Systems

Preprint

D.C. Jordan,[1] D.B. Sulas-Kern,[1] S. Johnston,[1]
H.R. Moutinho,[1] C. Xiao,[1] C.S. Jiang,[1] M. Young,[1]
A.G. Norman,[1] C. Deline,[1] I. Repins,[1] R. Bhoopathy,[2]
O. Kunz,[2] Z. Hameiri,[2] C. Sainsbury[3]

1 National Renewable Energy Laboratory
2 USNW Australia
3 Sinton Instruments

Suggested Citation
Jordan, D.C., D.B. Sulas-Kern, S. Johnston, H.R. Moutinho, C. Xiao, C.S. Jiang, M. Young, A.G. Norman, C. Deline, I. Repins, R. Bhoopathy, O. Kunz, Z. Hameiri, C. Sainsbury. 2020. *High Efficiency Silicon Module Degradation - From Atoms to Systems: Preprint*. Golden, CO: National Renewable Energy Laboratory. NREL/CP-5K00-77483. https://www.nrel.gov/docs/fy20osti/77483.pdf.

Conference Paper
NREL/CP-5K00-77483
September 2020

National Renewable Energy Laboratory
15013 Denver West Parkway
Golden, CO 80401
303-275-3000 • www.nrel.gov

NOTICE

This work was authored in part by the National Renewable Energy Laboratory, operated by Alliance for Sustainable Energy, LLC, for the U.S. Department of Energy (DOE) under Contract No. DE-AC36-08GO28308. Funding provided by the U.S. Department of Energy Office of Energy Efficiency and Renewable Energy (EERE) under Solar Energy Technologies Office (SETO) Agreement Number 30295. The views expressed herein do not necessarily represent the views of the DOE or the U.S. Government. The U.S. Government retains and the publisher, by accepting the article for publication, acknowledges that the U.S. Government retains a nonexclusive, paid-up, irrevocable, worldwide license to publish or reproduce the published form of this work, or allow others to do so, for U.S. Government purposes.

Cover Photos by Dennis Schroeder: (clockwise, left to right) NREL 51934, NREL 45897, NREL 42160, NREL 45891, NREL 48097, NREL 46526.

HIGH EFFICIENCY MODULE DEGRADATION – FROM ATOMS TO SYSTEMS

D.C. Jordan*[1], D.B. Sulas-Kern[1], S. Johnston[1], H.R. Moutinho[1], C. Xiao[1], C.S. Jiang[1], M. Young[1], A.G. Norman,[1], C. Deline[1], I. Repins[1], R. Bhoopathy[2], O. Kunz[2], Z. Hameiri[2], C. Sainsbury[3]
[1]National Renewable Energy Laboratory (NREL), 15013 Denver West Parkway., Golden, CO, USA
[2]SPREE, UNSW Sydney, Kensington, NSW, 2052, Australia
[3]Sinton Instruments, Boulder, CO 80301 USA

ABSTRACT: For photovoltaics (PV) to be cost competitive with traditional energy sources, reliability is of critical importance. Historically, PV reliability has focused on the module packaging because degradation and failure modes were directly linked to the packaging. Today, in addition to module packaging, cell related reliability issues can increasingly be observed. We have investigated PV systems of high-efficiency modules such as silicon heterojunction (HJ) and passivated emitter and rear cell (PERC). System degradation of these technologies is found to be no worse than systems using conventional cell technologies. Module performance loss, for HJ and PERC technologies, shows open-circuit voltage reduction indicative of cell level changes. For HJ modules, possible hydrogen concentration changes and a rougher interface between the amorphous silicon and the silicon is observed, although more samples are needed to confirm these findings. The PERC modules show hydrogen changes in the front and rear of the cell with more changes pronounced at the front. Importantly, these two case studies demonstrate that cell level understanding is required to accurately predict module and system performance for high-efficiency technologies.

1 INTRODUCTION

Today photovoltaics (PV) systems are cost competitive with traditional energy sources, however, efficiency and reliability are of vital importance [1]. Efficiency is important for obvious direct reasons, but has also an indirect benefit through reduced area, balance-of-systems (BOS), labor, materials requirements etc. However, the cost competitiveness is achieved over the life of the system, thus, reliability may not be as obvious, but can be equally important. Energy loss can be caused by underperformance and/or failures or disruptions at the system, module and cell level. Minimizing and understanding underperformance and failures at all levels are a vital part of PV reliability.

Traditionally, crystalline silicon (c-Si) system field degradation was dominated by losses in short-circuit current (I_{SC}) or fill factor (FF), depending on the underlying degradation mechanism [2]. As cells and modules have evolved towards their theoretical efficiency limits, more cell-related phenomena, such as light induced degradation (LID) or light and elevated temperature induced degradation (LeTID), manifested through open-circuit voltage (V_{OC}) losses, have been observed impacting modules and systems [3,4]. Despite the introduction of high-efficiency modules into the commercial market more than a decade ago, multi-year field studies of these technologies are not as common as desired [5,6].

In this paper we focus on two c-Si high-efficiency technologies, heterojunction (HJ) and passivated emitter and rear cell (PERC). We examine their performance loss from the system to the cell and nanoscale levels, linking overall energy output with fundamental materials changes during outdoor aging.

2 SYSTEM PERFORMANCE

In the PV Fleet Performance Data Initiative time series data are collected across the USA to assess the overall PV fleet performance and distill regional trends [7]. Figure 1 shows a cumulative distribution function of the performance loss rate by systems using high-efficiency modules such as PERC and HJ. The systems using PERC modules originated from one manufacturer. For comparison, conventional aluminum back surface field (Al-BSF) modules from the same manufacturer in a similar climate zone and mounting configuration are also shown. Each performance loss rate was determined from AC power data using satellite data for irradiance and RdTools as the methodology [8]. The uncertainty of the performance loss rate is indicated for each system by a horizontal line of the respective color. At the median, the performance loss rate for the PERC systems is slightly smaller than the Al-BSF equivalent. The positive tail of the PERC systems may be caused by the substantially shorter exposure time, measurement uncertainty and possible start-up problems that are fixed in time. The HJ systems show a slightly smaller performance loss rate possibly aided by more systems installed in cooler climates. Given this limited data set we do not observe performance loss rates that are atypical or uneconomical.

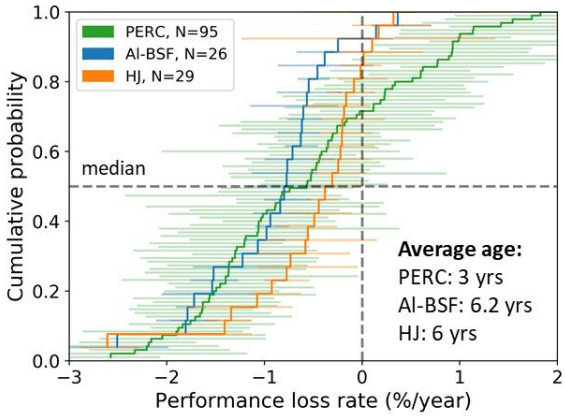

Figure 1: Cumulative distribution function of systems using PERC, Al-BSF and heterojunction cell technologies. Uncertainties of each performance loss rate is indicated by horizontal bar in respective colors. The average age for each category is given in the inset.

3 SILICON HETEROJUNCTION MODULES

Silicon heterojunction technology has received considerable attention not least because of record efficiency for c-Si cells [9]. As a commercial product, HJ are attractive because of fewer processing steps compared to a PERC manufacturing line, and advances in availability of low-cost high-quality n-type wafers, improvements in metallization etc. [10]. In the HJ structure, the n-type Si wafer is enveloped by a thin hydrogenated amorphous

silicon (a-Si:H) layer and capped by a transparent conducting oxide (TCO) because of poor lateral conductivity of a-Si. Other attractive features for field performance include the low temperature coefficient and a high bifacial factor [11]. Several field studies showed gradual Voc loss, hinting that cell changes take place, although the detected performance losses were generally within the warranty [12,13,14]. In this section we continue our investigation into the mechanisms of the V_{OC} loss and small series resistance (R_S) increase that we reported previously. The system under investigation was installed at the National Renewable Energy Laboratory (NREL), USA for ca. 10 years. In addition, to the fielded module we also had a control module that was kept indoors during the same time.

Figure 2: EL imaging of the fielded module at forward-

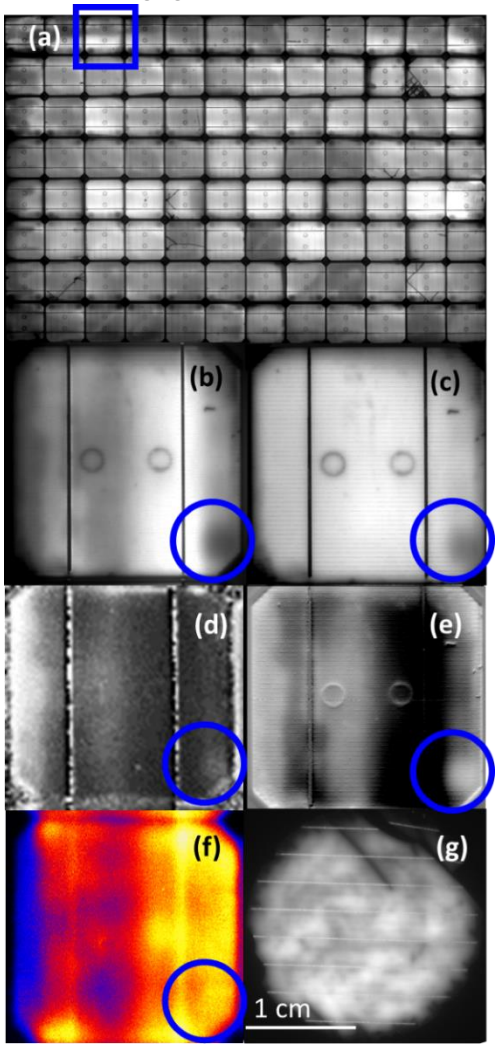

bias equivalent of I_{SC} (a). One of the cells selected for enlarged cell imaging by high-current EL (b), PL (c), line-scan PL/EL ratio (d) and low-/high-current ratio EL (e). Dark lock-in thermography of the same cell (f) and PL of a 3/4" cored piece from the cell (g). The blue circle highlights an area indicated by a darker region in El and PL but lighter contrast in the ratio image (d) and the area of the cored piece.

Figure 2(a) shows an electroluminescence (EL) image of one of the fielded modules at forward-bias equivalent of I_{SC} (+3.8A). A few cracked cells can be observed that were caused during transport to various characterization laboratories. These cells are not the causes of the observed degradation, as we have shown in previous characterization and can be ignored for the subsequent discussion. The blue highlighted cell is one example that is further explored with high-current EL and photoluminescence (PL) in Fig. 2(b)-(c). Regions across the cell that are dark in EL and bright in PL indicate resistance issues, and regions that are dark in both imaging techniques indicate degradation of material quality.

Figure 3: EL imaging of the fielded module at forward-

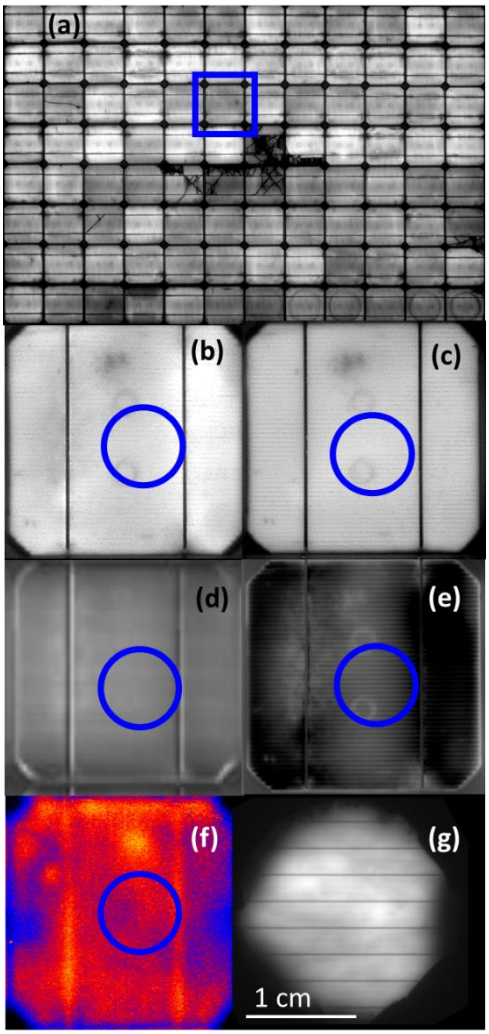

bias equivalent of I_{SC} (a). One of the cells selected for enlarged cell imaging by high-current EL (b), PL (c), line-scan PL/EL ratio (d) and low-/high-current ratio EL (e). Dark lock-in thermography of the same cell (f) and PL of a 3/4" cored piece from the cell (g). The blue circle highlights the area of the cored piece (e).

Figure 2(d) displays the same cell as the ratio between line-scan PL and EL that enhances R_S defects (brighter areas), while suppressing the lifetime related defects due to an inversion in luminescence intensity as reported in [15]. The ratio of low-/high-current EL is shown in Fig. 2(e), where low current is 0.1 times the forward-bias equivalent of I_{SC}. Similar to the line-scan PL example in Fig. 2(d), darker regions show less resistive impact. Dark lock-in thermography (DLIT) is another non-destructive characterization tool that shows cooler regions on the left-

hand side of the cell in Fig. 2(f) commensurate with the resistive areas that receive less current flow. The blue circle indicates an area that was physically removed from the cell for further materials characterization [16]. The successful extraction from the module is corroborated by the PL image of the cored section in Fig. 2(g). It is conceivable that the different regions across the cell visible in Fig. 2 may have different underlying degradation mechanisms.

The equivalent images for the control module are displayed in Fig. 3. It can be noted that the two ratio images, Fig. 3(d)-(e), show a generally darker shade than the fielded module, indicative of overall lower resistance. Additionally, it should be noted that at the same current injection, the luminescence intensity in the control module was approximately twice that of the fielded module, consistent with higher V_{OC} (lower loss) in the control. One of the cells that we further investigated is indicated by a blue rectangle, and the cored piece is indicated by a blue circle.

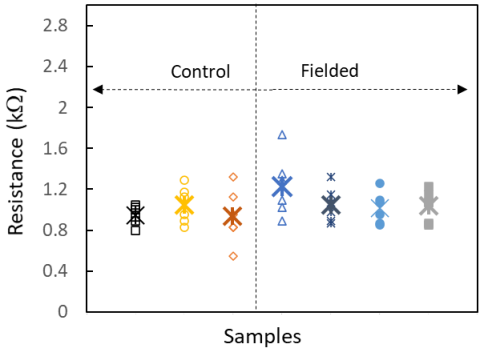

Figure 4: Scanning spreading resistance microscopy (SSRM) of cored pieces from the control (left) and fielded module (right). The average value for each sample is indicated by the cross.

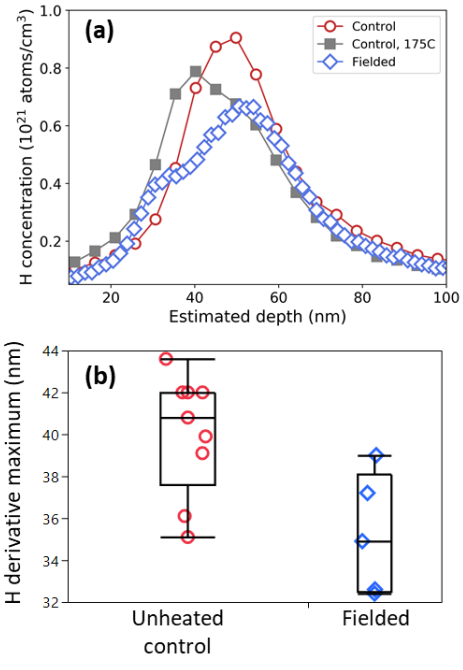

Figure 5: Hydrogen concentration from dynamic secondary ion mass spectroscopy traces for a fielded, control and a control sample that was heated to 175ºC for 20 hours (a). The maximum of hydrogen concentration derivative for control and fielded samples (b).

Because the TCO is integral for lateral conductivity in the HJ structure, we investigated whether the resistance of the TCO contributes to the overall higher R_S by scanning spreading resistance microscopy (SSRM). SSRM is a two-terminal resistance mapping technique based on an atomic force microscope (AFM). Because of the small probe contact area from the AFM tip, the current route decreases quickly away from the tip. Therefore, the resistance is dominated by the local TCO regardless of the current path through the underlying Si device. The results from several pieces of the fielded and control sample are depicted in Fig. 4. Substantial variation within a given sample can be seen for both sets of pieces, however no statistically significant difference between the fielded module and the control module can be discerned [17]. Thus, it appears that the conductivity of the TCO did not degrade during the 10-year field exposure, despite the apparent increase in Rs at the module level.

Several cored samples from the fielded and control module were investigated by dynamic secondary ion mass spectroscopy (d-SIMS). Figure 5(a) shows the hydrogen (H) concentration for a fielded (blue diamonds), a control (red circles) and a control sample that was heated to 175ºC for 20 hours (grey squares). Because of the texturing of the Si wafer, the sample orientation relative to the d-SIMS sputtering beam can have considerable impact on the profile shape and location of the profile maximum. However, these samples were aligned with similar sample orientation for best comparison. The fielded sample exhibits a secondary peak especially compared to the control sample trace. The heated control sample also appears to exhibit a shoulder that could indicate a secondary peak. We plan to continue d-SIMS studies to further determine the degree to which the secondary peak is related to texturing effects versus whether a real re-distribution of hydrogen occurs to account for the change in H profile that we observe.

To determine the location of the secondary H concentration peak, the derivative for all unheated control samples is contrasted against samples from the fielded module in Fig. 5(b). The depth of H concentration for the fielded samples is statistically significant and less than for the unheated control samples at a p-value of 0.01. However, the sample orientation was not the same for all samples. Therefore, despite the significance, more samples and careful alignment of the incident sputtering beam with respect to the pyramid texture orientation are required to confirm this difference, which could indicate a possible H re-distribution in the sample.

Finally, Fig. 6 displays high-resolution transmission electron microscopy (TEM) images of the fielded and control module that show the physical structure of the electrical junction. The a-Si:H layer is sandwiched between the c-Si wafer and the multicrystalline TCO. The root mean square (RMS) roughness of the a-Si:H/c-Si interface indicates that the interface may be rougher for the fielded sample compared to the control and recent high-efficiency cells [18]. However, the TEM contrast, especially for the fielded module is not as high as desired because surface texture the facets on the Si wafer are not exactly parallel to the {111} planes and made alignment in

the TEM difficult. Therefore, more cross-sectional samples will be characterized to corroborate the current findings and their role in the energy loss in these types of modules. Yet, this case study is a good demonstration how cell phenomena at the atomic level can have considerable impact at the macroscopic level.

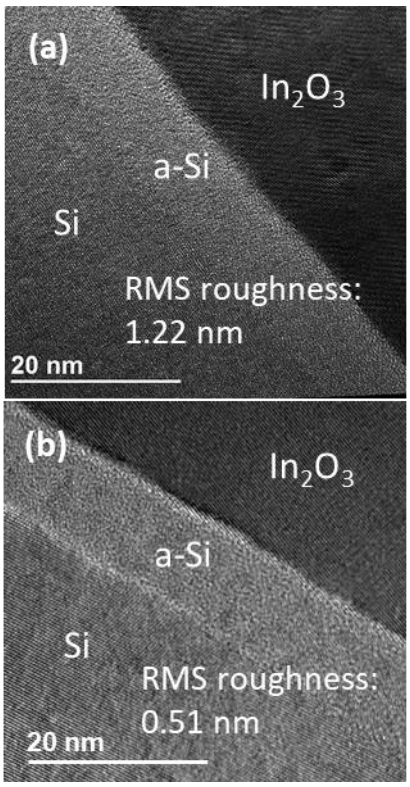

Figure 6: Cross section transmission electron microscopy images of the fielded (a) and the control module (b). The root mean square (RMS) roughness at the a-Si:H/Si interface is also given.

4 PERC MODULES

The second case study of the synergistic nature of cell, module and system level involves PERC modules from a different manufacturer. Although the PERC structure was first reported in 1989 it has found its way into commercial products only in the last decade [19]. Monofacial PERC, bifacial PERC, and Al-BSF modules and equivalent strings of the same type were installed at NREL for 2-3 years. Both PERC modules were packaged in a glass-glass construction whereas the Al-BSF had a glass-backsheet construction. A bifacial PERC control module was kept indoors during the same time. Performance loss rates for individual current-voltage parameters are shown in Fig. 7. The maximum power (P_{MAX}) loss for the Al-BSF module is in the typical historical range and the loss is roughly divided between short-circuit current (I_{SC}) and fill factor (FF) depending on the underlying degradation mechanism. In addition, no open-circuit voltage (V_{OC}) loss is also typically observed for this technology. The monofacial PERC module shows similar P_{MAX} loss as the Al-BSF module but V_{OC} loss is now clearly visible.

The bifacial PERC module also shows V_{OC} loss but exhibits additional I_{SC} and FF loss leading to a slightly higher overall performance loss. Indoor measurements (filled symbols) confirm the outdoor measurements (open symbols). Lifetime curves taken from Suns-V_{OC} measurements for these 3 modules are shown in Fig. 7(b). At Pmax the lifetime between the modules is very similar but at higher injection levels the PERC modules show considerably lower lifetimes corroborating the V_{OC} loss.

EL and PL imaging, Fig. 8, shows no obvious defects such as cracked cells, thus the V_{OC} loss may indicate again cell level problems. The bifacial module exhibits resistive regions (red circle) and areas of material quality issue (blue circle) similar to the HJ modules. In contrast, the monofacial module shows mostly resistive areas indicated by slight darkening in areas of the EL but more uniformly bright in PL. Subsequently, samples from these modules were cored for further materials characterization. Because of the glass-glass package, the extraction was more challenging than for glass-backsheet constructions resulting in smaller samples. However, the areas were large enough to allow for d-SIMS measurements.

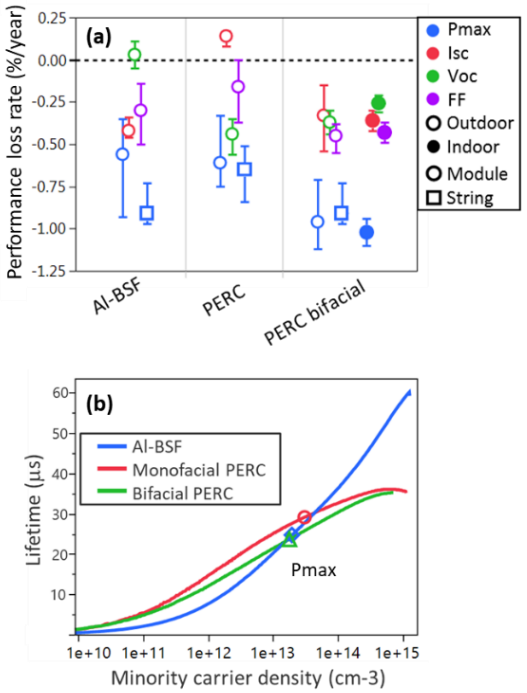

Figure 7: Performance loss rates for Al-BSF, monofacial PERC and bifacial PERC modules and strings from manufacturer B (a). Lifetime curves obtained from Suns-V_{OC} measurements (b).

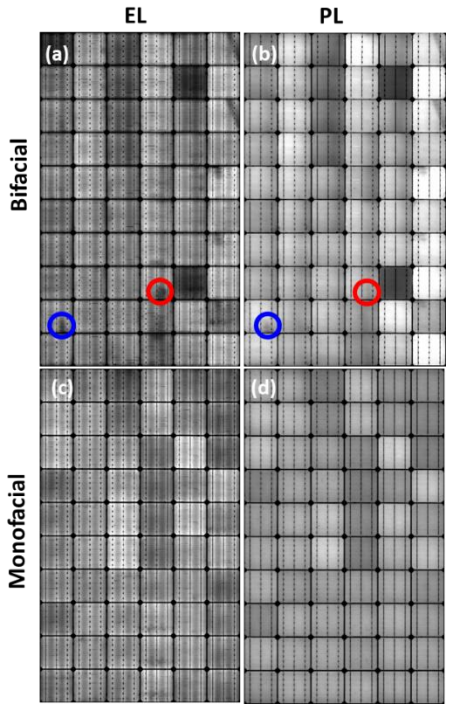

Figure 8: EL (a, c) and PL (b, d) images for bifacial (top) and monofacial (bottom) PERC modules. Red and blue circles indicate resistive problems (dark in EL and bright in PL) and material issues (dark in EL and PL), respectively.

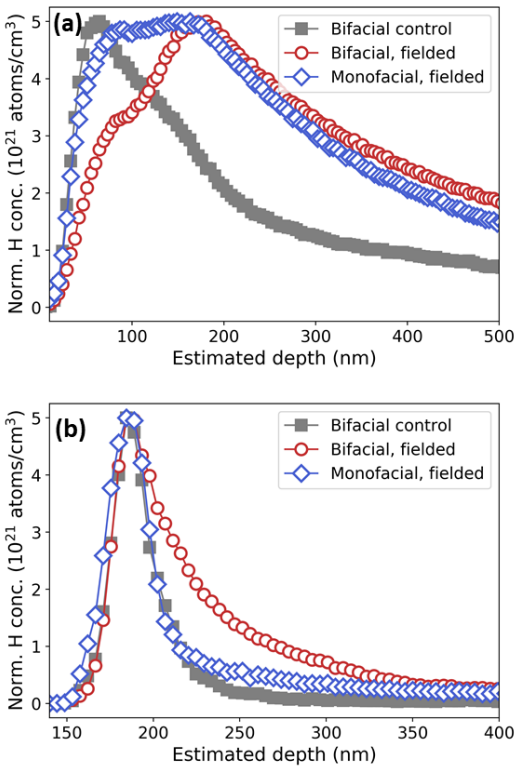

Figure 9: D-SIMS traces of H concentration for the PERC module from the front (a) and the back (b).

The hydrogen concentration is shown for the bifacial control (grey squares), the fielded bifacial (red circles), and the fielded monofacial module (blue diamonds) from the front in Fig. 9(a) and the back in Fig. 9(b). The sample orientation for all samples was fixed with respect to the fingers to minimize texturing artifacts, and the concentration normalized to the maxima. At the front surface, the bifacial control sample shows a pronounced H peak that slowly declines into the bulk of the cell. In contrast, fielded bifacial sample shows a secondary peak and a much broader distribution into the bulk. The monofacial sample shows a broader peak and distributions that is broader than the bifacial control but not as wide as the fielded bifacial sample. This data suggests that H may diffuse into the bulk of the cell. At the back, we see a similar pattern for all 3 samples, although not as pronounced as on the front of the cell. This further suggests that H may be re-distributed in the fielded modules compared to the control module.

6 CONCLUSIONS

We have investigated PV systems comprised of high-efficiency modules such HJ and PERC. System degradation of these technologies was found to be no worse than systems using conventional cell technologies. Module performance loss for both technologies show V_{OC} loss indicating cell level changes. For HJ, possible hydrogen distribution changes and a rougher a-Si:H/c-Si interface were observed, although more samples need to be analyzed to confirm these findings. The PERC modules similarly appear to show hydrogen changes in the front and rear of the cell, although the changes appear more pronounced at the front. More samples are needed to validate these findings. Finally, these two case studies demonstrate that cell and materials level understanding is helpful performance for high-efficiency technologies.

7 ACKNOWLEDGEMENTS

The authors would like to thank the PV Fleet group, Michael Deceglie, Kevin Anderson, Kirsten Perry, Robert White, Martin Green, Stefan DeWolf, Zach Holman, Mariana Bertoni, Robert Flottenmesh, Katherine Jordan. This work was authored in part by Alliance for Sustainable Energy, LLC, the manager and operator of the National Renewable Energy Laboratory for the U.S. Department of Energy (DOE) under Contract No. DE-AC36-08GO28308. Funding provided by the U.S. Department of Energy's Office of Energy Efficiency and Renewable Energy (EERE) under Solar Energy Technologies Office

(SETO) Agreement Number 30295. The views expressed in the article do not necessarily represent the views of the DOE or the U.S. Government. The U.S. Government retains and the publisher, by accepting the article for publication, acknowledges that the U.S. Government retains a nonexclusive, paid-up, irrevocable, worldwide license to publish or reproduce the published form of this work, or allow others to do so, for U.S. Government purposes.

8 REFERENCES

[1] EIA (2020). Annual Energy Outlook 2020 with Projections to 2050. (No. AEO2020).

[2] D.C. Jordan, J.H. Wohlgemuth, S.R Kurtz, Technology and Climate Trends in PV Module Degradation, 27th European Photovoltaic Solar Energy Conference, Frankfurt, Germany, (2012), 3118 - 3124.

[3] B. Hallam, M. Abbott, J. Bilbao, P. Hamer N. Gorman, M. Kim, D. Chen, K. Hammerton, D. Payne, C. Chan,N. Nampalli, S. Wenham., Energy Procedia, 92, (2016), 42 ¬ 51

[4] F. Kersten, P. Engelhart, H.-C. Ploigt, A. Stekolnikov, T. Lindner, F. Stenzel, M. Bartzsch, A. Szpeth, K. Petter, J. Heitmann, J.W. Müller, A New mc-Si Degradation Effect called LeTID, 42nd IEEE Photovoltaic Specialists Conference, New Orleans, LA, 2015

[5] D.C. Jordan, C. Deline, M. Deceglie, T.J. Silverman, W. Luo, PV Degradation – Mounting & Temperature, 46th IEEE Photovoltaic Specialists Conference, Chicago, IL, USA, 2019.

[6] M.G. Deceglie , T.J. Silverman, S.W. Johnston, J.A. Rand , M.J. Reed, R. Flottemesch, I.L. Repins, Light and Elevated Temperature Induced Degradation (LeTID) in a Utility-Scale Photovoltaic System, IEEE Journal of Photovoltaics, 10 (4) (2020), 1084.

[7] C. Deline, R. White, M. Muller, K. Anderson, K. Perry, M. Deceglie, L. Simpson, D. Jordan, M. Bolinger PV Fleet Performance Data Initiative Program and Methodology, 46th IEEE Photovoltaic Specialists Conference, Chicago, IL, USA, 2019.

[8] D. Jordan, C. Deline, S. Kurtz, G. Kimball, M. Anderson, Robust PV Degradation Methodology and Application, IEEE Journal of Photovoltaics, 8(2) (2018), 525-531.

[9] K. Yoshikawa, H. Kawasaki,W. Yoshida, T. Irie, K. Konishi, K. Nakano, T. Uto, D. Adachi, M. Kanematsu, H. Uzu, K. Yamamoto, "Silicon heterojunction solar cell with interdigitated back contacts for a photoconversion efficiency over 26%", Nature Energy, 2, (2017), 17032.

[10] C. Ballif, M. Boccard, A. Descoeudres, C. Allebé, A. Faes, O. Dupré, J. Haschke, P.-J. Ribeyron, M. Despeisse, Solving all bottlenecks for silicon heterojunction technology, PV International, (2019).

[11] S. DeWolf, A. Descoeudres, Z.C. Holman, C. Ballif, High-efficiency Silicon Heterojunction Solar Cells: A Review, Green, 2 (2012), 7–24

[12] D.C. Jordan , C. Deline , S. Johnston, S.R. Rummel, B.Sekulic, P. Hacke , S.R. Kurtz , K.O. Davis , E.J. Schneller , X.Sun , M.A. Alam, R.A. Sinton, Silicon Heterojunction System Field Performance, IEEE Journal of Photovoltaics, 8(1), (2018), 177 182.

[13] T. Ishii, A. Masuda, Annual degradation rates of recent crystalline silicon photovoltaic modules, Progress in Photovoltaics, 25(12), (2017), 953967.

[14] W. Luo, Y. Sheng K., P. Hacke, D. Jordan, L. Zhao, S. Ramakrishna, A.G. Aberle, T. Reindl, Analysis of the long-term performance degradation of crystalline silicon photovoltaic modules in tropical climates, Journal of Photovoltaics, 9(1), (2019), 266 ¬ 271.

[15] I. Zafirovska, M. K. Juhl, J. W. Weber, J. Wong, T. Trupke, "Detection of Finger Interruptions in Silicon Solar Cells Using Line Scan Photoluminescence Imaging," IEEE Journal Photovoltaics, 7(6), (2017), 1496–1502.

[16] H. Moutinho, B. To, D. Sulas-Kern, C.S. Jiang, M. Al-Jassim, S. Johnston, Advances in Coring Procedures of Silicon Photovoltaic Modules, 47th IEEE Photovoltaic Specialists Conference, virtual, 2020.

[17] C.-S. Jiang, D.B. Sulas-Kern, H.R. Moutinho, D.C. Jordan, C. Xiao, S. Johnston, and M.M. Al-Jassim, Local resistance measurement for degradations of c-Si heterojunction with intrinsic thin layer (HIT) solar modules, 47th IEEE Photovoltaic Specialists Conference, virtual, 2020.

[18] X. Ru, M. Qu, J. Wang, T. Ruan, M. Yang, F. Peng, W. Long, K. Zheng, H. Yan, X. Xu, 25.11% efficiency silicon heterojunction solar cell with low deposition rate intrinsic amorphous silicon buffer layers, Solar Energy Materials and Solar Cells, 215, (2020).

[19] M.A. Green, The Passivated Emitterand Rear Cell (PERC): From conception to mass production, Solar Energy Materials & Solar Cells, 143, (2015), 190-197.